Defect-Induced Magnetism in Neutron Irradiated 6*H*-SiC Single Crystals

Yu Liu,[1] Gang Wang,[1,*] Shunchong Wang,[1] Jianhui Yang,[2] Liang Chen,[2] Xiubo Qin,[3] Bo Song,[4] Baoyi Wang,[3] and Xiaolong Chen[1,†]

[1]*Research & Development Center for Functional Crystals, Beijing National Laboratory for Condensed Matter Physics, Institute of Physics, Chinese Academy of Sciences, Post Office Box 603, Beijing 100190, China*
[2]*Ningbo Institute of Material Technology & Engineering, Chinese Academy of Sciences, Ningbo 315201, China*
[3]*Institute of High Energy Physics, Chinese Academy of Sciences, Beijing 100049, China*
[4]*Academy of Fundamental and Interdisciplinary Sciences, Harbin Institute of Technology, Harbin 150080, China*
(Received 7 August 2010; published 24 February 2011)

Defect-induced magnetism is firstly observed in neutron irradiated SiC single crystals. We demonstrated that the intentionally created defects dominated by divacancies ($V_{Si}V_C$) are responsible for the observed magnetism. First-principles calculations revealed that defect states favor the formation of local moments and the extended tails of defect wave functions make long-range spin couplings possible. Our results confirm the existence of defect-induced magnetism, implying the possibility of tuning the magnetism of wide band-gap semiconductors by defect engineering.

DOI: 10.1103/PhysRevLett.106.087205 PACS numbers: 75.50.Pp, 71.15.Mb, 71.55.−i, 75.50.Dd

It is well known that localized magnetic moments and the coupling between them are two indispensable factors to induce long-range spin ordering in solids, exhibiting ferromagnetism (FM), antiferromagnetism (AFM), ferrimagnetism, etc. The local spins usually come from the elements containing the partially filled $3d$ or $4f$ subshells, where the electron configuration favors the high-spin states according to the Hund's rule. The coupling strength between the spins depends on the exchange integral that is sensitive to the separation of the spins. Coupling over a large separation is possible as evidenced by diluted magnetic semiconductors, where the concentrations of $3d$ metals are only several percents. The itinerant carriers are thought to play a role in mediating spin orientations between magnetic atoms. Recently, more interest has focused on the magnetism in wide band-gap (WBG) semiconductors as the Curie temperatures can be attained at around room temperature (RT) by dopings, which is important for applications in spintronics [1–7]. Limited solubility of $3d$ metals in WBG semiconductors, however, often leads to the precipitation of second phases, thwarting the attempts to get the unambiguous experimental results [2,8]. So, study on the low solubility regime is preferred. Yet, the separation of contributions to the observed magnetism from magnetic elements and other sources still remains difficult.

On the other hand, there has been increasing evidence that traditional magnetic elements are not the sole source in inducing intrinsic magnetism; for a recent review see Ref. [9]. RT FMs were observed in highly oriented pyrolytic graphite (HOPG) [10–12], in Al doped SiC [13], in Li doped ZnO [14], and in various nanosized compounds [15,16] that are otherwise nonmagnetic in their bulk states. Theoretical studies revealed that the local moment can form from defects and the extended tails of their wave functions mediate long-range magnetic coupling [17–22]. In this Letter, we provide convincing experimental evidence that defects can induce magnetism in clean single crystals. The results on the magnetic properties of 6*H*-SiC single crystals containing intentionally created defects by neutron irradiations under various doses are reported. It is demonstrated that defects, most of which are $V_{Si}V_C$, are the origin to the observed magnetism by carefully ruling out other possible sources and comparing the results with that of their pristine counterparts. First-principles calculations confirm that local moments are due to the defect sp states and the couplings are very long-range. Our study not only verifies the previous theoretical predictions [18–20,22] but also shows the possibility of tuning the magnetization of WGB semiconductors by defect engineering.

Commercially available 2 in semi-insulating p-type 6*H*-SiC (0001) wafer (TankeBlue, Beijing) was cut into pieces with dimensions of $10 \times 5 \times 0.33$ mm^3 for performing neutron irradiations. The measurement of the x-ray rocking curve confirmed the high crystalline quality of the wafer [full width half maximum (FWHM) is 21.6 arcsec]. The total concentration of main magnetic impurities (Fe, Co, Ni, Cr, and Mn, etc.) measured by secondary ion mass spectroscopy is below 3×10^{14} cm^{-3}. Other main impurities are B (5.66×10^{17} cm^{-3}), Al (1.33×10^{16} cm^{-3}), N (2.99×10^{17} cm^{-3}), and V (7.82×10^{15} cm^{-3}). Under a temperature less than 50 °C, the irradiations were carried out with neutrons at a dose rate of 2.65×10^{13} n/cm^2 s and the dose rate due to thermal neutrons and fast neutrons were 2.0×10^{13} n/cm^2 s and 6.5×10^{12} n/cm^2 s, respectively. Samples were divided into four groups and irradiated for varying durations, corresponding doses in the ranges of 1.91×10^{17}–2.29×10^{18} n/cm^2. Each piece was irradiated only once and pristine pieces taken from the same wafer were kept for the purpose of comparison.

 © 2011 American Physical Society

We first examined the crystallinity of the samples after neutron irradiations. Raman spectra in Fig. 1(a) show that the patterns of 6*H*-SiC crystals irradiated by varying neutron doses are similar to that of the pristine one. There are no other SiC polytypes or secondary phases detected under the sensitivity of Raman characterization. The main difference among the patterns is the decrease in intensity for each mode with increasing irradiation dose. Figure 1(b) displays the relative intensity variation of the folded longitudinal optical (FLO) mode given by $(1 - I/I_0)$ vs irradiation dose, where I_0 and I are the intensities of the peak measured in the pristine and irradiated samples, respectively. Such a change in relative intensity suggests the existence of defects or lattice damages [23] in the irradiated samples though there is no noticeable change in FWHM of x-ray rocking curves.

To investigate the defect types and their concentrations created by the neutron beam, we performed a series of measurements by positron annihilation lifetime spectroscopy (PALS). A lifetime spectrum is a linear combination of exponential functions corresponding to different annihilation sites. As a rule, we fit all the measured spectra into an exponential function of three components. A long lifetime of about 2000 ps corresponding to annihilations at voids or sample surface is found to be very small in its fraction as usual [24] and we do not consider it in the following analysis. The fitted two remaining positron lifetimes τ_1, τ_2, and the fraction of the longer lifetime (τ_2) component I_2 as functions of irradiation dose are shown in Fig. 2. It is found that the lifetimes τ_1 and τ_2, taking values of 130 ± 14 ps and 239 ± 20 ps, are independent of irradiation dose, while I_2 is closely correlated with irradiation dose. The lifetime value of 130 ± 14 ps, similar to the prior experimental [25–27] and theoretical values [28], is attributed to the bulk lifetime of 6*H*-SiC. The positron trapping center at 239 ± 20 ps, close to 253 ± 4 ps [25] and 225 ± 11 ps [27], is defect related and corresponding to defects dominated by $V_{\mathrm{Si}}V_{\mathrm{C}}$ in *p*-type 6*H*-SiC crystals. The dependence of I_2 on irradiation dose reveals that the concentration of $V_{\mathrm{Si}}V_{\mathrm{C}}$ increases with the increasing irradiation dose, in accordance with the Raman scattering data. The PALS measurements show that $V_{\mathrm{Si}}V_{\mathrm{C}}$ is created by neutron irradiations and confirm that its concentration is enhanced by increasing dose. In our case, the concentration of $V_{\mathrm{Si}}V_{\mathrm{C}}$ was roughly estimated to be 4.3×10^{17} cm^{-3} at the largest dose of 2.29×10^{18} n/cm^2 assuming that the pristine crystal's concentration is 4.1×10^{16} cm^{-3} [27].

The magnetization measurements were performed with a superconducting quantum interference device vibrating sample magnetometer which features a sensitivity of 10^{-7} emu. Figure 3(a) shows the variations of magnetization with applied field in the range of -5 KOe $< H <$ 5 KOe at 5 K. It is noticed that only diamagnetic (DM) features can be observed in the pristine sample. After a low dose irradiation of 1.91×10^{17} n/cm^2, the sample's DM features are becoming weaker and a minor hysteresis loop can be seen in low magnetic field range. With increasing irradiation dose, the magnetic order gradually enhances and DM *M*-*H* features further weaken, accompanied by an anticlockwise rotation of the hysteresis loops. Finally, at a dose of 2.29×10^{18} n/cm^2, a distinct hysteresis loop with ferromagnetic features as indicated in Fig. 3(b) can be clearly seen and the saturation magnetization reaches 1×10^{-4} emu/g, which is ~23 times larger than 4.3×10^{-6} emu/g, the maximum value possibly induced by the magnetic impurities in the used SiC crystals in this study. Even at 300 K, hysteresis loop can still be observed as shown in Fig. 3(c) with saturation magnetization of about 2×10^{-5} emu/g. (Note that the FM is not homogeneously distributed but probably exists in domains. The magnetization values obtained by dividing the magnetic moment by the total mass do not correspond to the expected intrinsic values.) The observed hysteresis loops demonstrate that intrinsic magnetism is definitely induced by neutron irradiations.

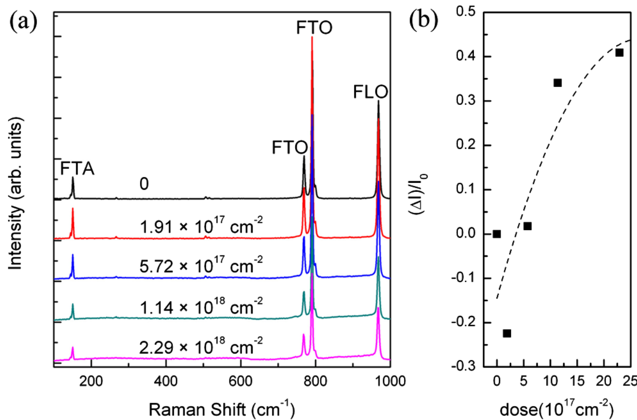

FIG. 1 (color online). (a) Raman spectra from 100 cm^{-1} to 1000 cm^{-1} for irradiated and pristine SiC samples. (b) The relative intensity of the FLO mode versus irradiation dose. The dashed line is a guide to the eyes.

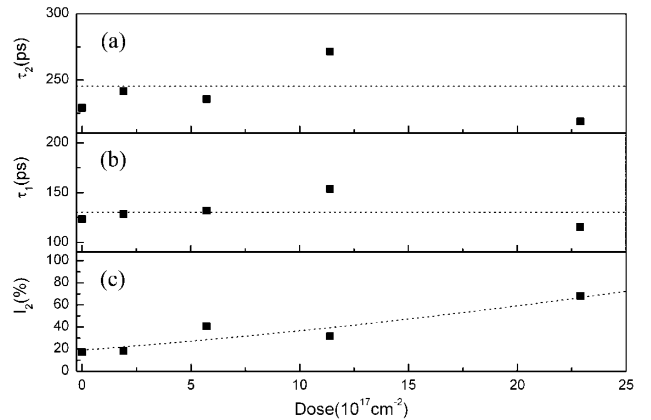

FIG. 2. Fitted results of τ_2 (a), τ_1 (b) and I_2 (c) as functions of irradiation dose. τ_1 and τ_2 are found to be independent of dose. I_2 is proved to have positive correlation with dose. The dotted line shows the average values in (a) and (b) while is a guide to the relationship between I_2 and irradiation dose in (c).

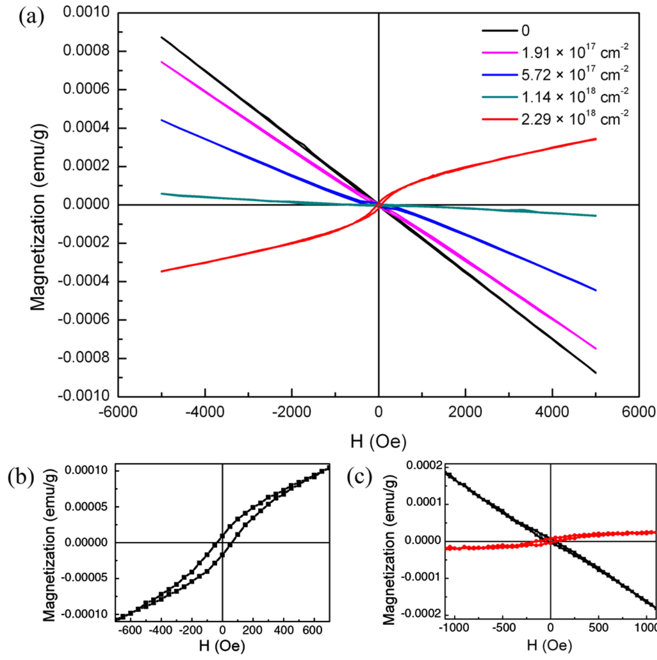

FIG. 3 (color online). (a) The magnetization (in units of $1\ \text{emu} = 10^{-3}\ \text{A}\,\text{m}^2$) measured at $T = 5$ K as a function of magnetic field ($1\ \text{Oe} = 10^3/4\pi\ \text{A}\,\text{m}^{-1}$) in the range $-5\ \text{KOe} < H < 5\ \text{KOe}$ for irradiated and pristine SiC samples. (b) The magnified hysteresis loop for the sample with dose of $2.29 \times 10^{18}\ n/\text{cm}^2$ at $T = 5$ K. (c) The magnetic signals with (black) and without (red) the DM contribution in low magnetic field range for the sample with dose of $2.29 \times 10^{18}\ n/\text{cm}^2$ at $T = 300$ K.

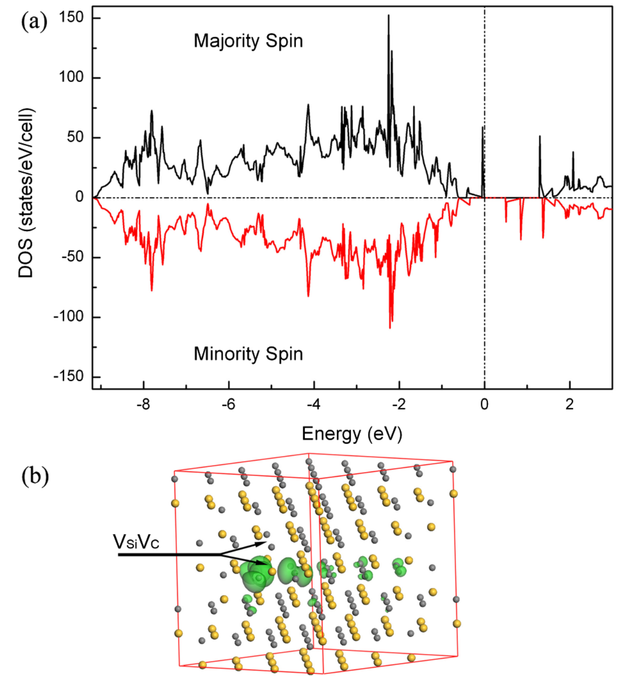

FIG. 4 (color online). (a) Spin-resolved DOS of a neutral $V_{\text{Si}}V_{\text{C}}$ in a 192-atom SiC supercell. The spin polarization leads to a splitting between two kinds of spin states. (b) Isosurface charge density plot (isovalue is $0.02\ e/\text{Å}^3$) of the total spin states about a neutral $V_{\text{Si}}V_{\text{C}}$ in a 192-atom SiC supercell, showing both the localized nature and the extended tails of the defect wave functions. Si atoms are shown in yellow and C atoms in gray. Arrows indicate the location of $V_{\text{Si}}V_{\text{C}}$.

The similar variations of the divacancy concentration and the saturation magnetization with increasing irradiation dose suggest that the magnetism in neutron irradiated $6H$-SiC is closely associated with $V_{\text{Si}}V_{\text{C}}$. To understand the origin of the observed magnetism, we carried out first-principles calculations based on spin-polarized density-functional theory. All the calculations were performed by using the generalized gradient approximation in the form of the Perdew-Burke-Ernzerhof function [29], which was implemented in the Vienna *ab initio* simulation package [30]. Self-consistent field calculations were performed using projector augmented wave pseudopotentials with the cutoff energy set to 310 eV [31]. A supercell consisting of $4 \times 4 \times 1$ unit cells of $6H$-SiC containing one axial $V_{\text{Si}}V_{\text{C}}$ [$\text{Si}_{95}(V_{\text{Si}})\text{C}_{95}(V_{\text{C}})$], corresponding to a defect concentration of 0.5%, was built for calculations. (Note that this structure is studied only for obtaining the relationship between magnetism and defects and shall not be considered to represent a realistic distribution of defects.) The calculated spin-resolved density of states (DOS) of the 192-atom supercell [see Fig. 4(a)] shows that each neutral $V_{\text{Si}}V_{\text{C}}$ yields a magnetic moment of $2.0\mu_B$, consistent with the previous report [32]. Using this value, the numbers of the moments involved in FM and paramagnetism related to $V_{\text{Si}}V_{\text{C}}$ were estimated to be $3.5 \times 10^{16}\ \text{cm}^{-3}$ and $6.7 \times 10^{17}\ \text{cm}^{-3}$, respectively. The total number $7.0 \times 10^{17}\ \text{cm}^{-3}$ agrees with the estimated number of moments ($8.6 \times 10^{17}\ \text{cm}^{-3}$) created by $V_{\text{Si}}V_{\text{C}}$ based on PALS measurements, confirming the correlation of the magnetism with the divacancies. The spin-polarization energy, which is defined as the energy difference between the spin-polarized and spin-unpolarized states, was calculated to be 1.90 eV suggesting the spin-polarized state stable well above RT [19]. The spin polarization induced by the neutral $V_{\text{Si}}V_{\text{C}}$ leads to a 0.50 eV splitting between the majority- and minority-spin states. It should be pointed out that the splitting energy correction is not included here due to the consistency between the current calculation and the observation [33]. Figure 4(b) shows the charge density isosurface of defect states associated with a neutral $V_{\text{Si}}V_{\text{C}}$ in the 192-atom supercell. It demonstrates both the localized nature and the extended tails of the defect wave functions beyond the supercell, similar to the calculated results in vacancy-containing III-nitrides [19].

The extended tails of the defect wave functions will induce the long-range coupling between the moments caused by $V_{\text{Si}}V_{\text{C}}$. Following the calculating scheme by Dev *et al.* [19], we doubled the size of the supercell by putting two 192-atom cells side by side and attempted to study the magnetic coupling (FM or AFM) between the $V_{\text{Si}}V_{\text{C}}$-induced local moments. (Note that this antiferromagnetic structure is designed only for obtaining the

TABLE I. Magnetic coupling between $V_{Si}V_C$-induced local moments in 6H-SiC. The coupling is antiferromagnetic between two neutral $V_{Si}V_C$. Upon charging the defects entirely, the coupling becomes ferromagnetic.

Charge state	$E_{AFM} - E_{FM}$ (meV)	J_0 (meV)
(0, 0)	−78.8	−9.8
(+1, +1)	16.8	8.4
(−1, −1)	68.2	34.1

magnetic interaction.) The energy difference between the antiferromagnetic and ferromagnetic phases is $E_{AFM} - E_{FM} = 8J_0S^2$ according to the nearest-neighbor Heisenberg model, where J_0 is the nearest-neighbor magnetic coupling and S is the net spin of the defect states. A negative J_0 means that AFM is energetically favored and otherwise FM favored. As shown in Table I, the neutral $V_{Si}V_C$ couple antiferromagnetically with a separation of adjacent divacancies 12.3 Å. While for (+1, +1) and (−1, −1) charge states, we obtain ferromagnetic couplings with the identical separation. The varying values of J_0 for different charge states represent the different localized levels of the wave function, while the much larger value of J_0 for (−1, −1) charge state suggests that the electronic structure is more delocalized. Charging the divacancies is found to be favorable for promoting the magnetic coupling between the $V_{Si}V_C$-induced local moments. In our case, charging is probable as B acceptors and N donors with a level of $\sim 10^{17}$ cm^{-3} exist in the samples, with former's concentration a little bit higher. In addition, if the charge concentration is less than the divacancy density, this means that $V_{Si}V_C$ will be partially charged. Charged $V_{Si}V_C$ and neutral $V_{Si}V_C$ side by side may exist in some domains. We calculated the exchange interaction and found J_0 is −19.1 meV for (0, +1) and 9.8 meV for (0, −1) if assuming that the spins of $V_{Si}V_C$ are all the same in this case, suggesting partially charged divacancies also favor inducing spin ordering. The strong antiferromagnetic interaction for (0, +1) charge state implies $V_{Si}V_C$ charged by this way is not significant, if any, in our samples.

So far, we have studied the magnetic properties of semi-insulating p-type 6H-SiC with neutron irradiations. Many other techniques, including proton irradiation, ion implantation, electron bombardment, quick quenching, etc., might also alter the concentration or charge state of defects in SiC crystals, and hence induce the magnetization. In fact, some of the techniques have been successfully used to induce FM in HOPG [10–12]. It will be very interesting to obtain magnetic SiC and other WBG semiconductors with transition temperatures around or even above RT by these techniques.

In conclusion, we carefully study the defects and magnetism in 6H-SiC single crystals irradiated by varying doses of neutrons. $V_{Si}V_C$ are found to dominate in defects in crystals after irradiations. Our results unambiguously verify that defects can induce magnetism. The localized nature of the defect sp states foster the formation of local moments whereas the extended tails of the defect wave functions induce the long-range coupling between the moments caused by $V_{Si}V_C$. The results show the possibility of tuning the magnetization of SiC and other WBG semiconductors through defect engineering.

This work was partly supported by MOST under Grant Nos. 2006AA03A146, 2007BAE34B00, and 2009ZX02301, NSFC under Grant Nos. 90922037 and 51072222, and BMSTC under Grant No. D09080300500000.

*gangwang@iphy.ac.cn
†chenx29@iphy.ac.cn

[1] T. Dietl *et al.*, Science **287**, 1019 (2000).
[2] J. Y. Kim *et al.*, Phys. Rev. Lett. **90**, 017401 (2003).
[3] H. Saito *et al.*, Phys. Rev. Lett. **90**, 207202 (2003).
[4] S. B. Ogale *et al.*, Phys. Rev. Lett. **91**, 077205 (2003).
[5] M. Venkatesan *et al.*, Phys. Rev. Lett. **93**, 177206 (2004).
[6] S. Dhar *et al.*, Phys. Rev. Lett. **94**, 037205 (2005).
[7] W. Pacuski *et al.*, Phys. Rev. Lett. **100**, 037204 (2008).
[8] D. C. Kundaliya *et al.*, Nature Mater. **3**, 709 (2004).
[9] O. Volnianska and P. Boguslawski, J. Phys. Condens. Matter **22**, 073202 (2010).
[10] P. Esquinazi *et al.*, Phys. Rev. Lett. **91**, 227201 (2003).
[11] H. H. Xia *et al.*, Adv. Mater. **20**, 4679 (2008).
[12] X. M. Yang *et al.*, Carbon **47**, 1399 (2009).
[13] B. Song *et al.*, J. Am. Chem. Soc. **131**, 1376 (2009).
[14] J. B. Yi *et al.*, Phys. Rev. Lett. **104**, 137201 (2010).
[15] M. A. Garcia *et al.*, Nano Lett. **7**, 1489 (2007).
[16] A. Sundaresan and C. N. R. Rao, Nano Today **4**, 96 (2009).
[17] P. O. Lehtinen *et al.*, Phys. Rev. Lett. **93**, 187202 (2004).
[18] T. Chanier *et al.*, Phys. Rev. Lett. **100**, 026405 (2008).
[19] P. Dev, Y. Xue, and P. H. Zhang, Phys. Rev. Lett. **100**, 117204 (2008).
[20] H. W. Peng *et al.*, Phys. Rev. Lett. **102**, 017201 (2009).
[21] H. Lee, Y. Miyamoto, and J. Yu, Phys. Rev. B **79**, 121404 (2009).
[22] M. W. Zhao, F. C. Pan, and L. M. Mei, Appl. Phys. Lett. **96**, 012508 (2010).
[23] A. Pérez-Rodríguez *et al.*, J. Electron. Mater. **25**, 541 (1996).
[24] C. C. Ling, C. D. Beling, and S. Fung, Phys. Rev. B **62**, 8016 (2000).
[25] W. Puff *et al.*, Appl. Phys. A **61**, 55 (1995).
[26] S. Dannefaer, D. Craigen, and D. Kerr, Phys. Rev. B **51**, 1928 (1995).
[27] C. C. Ling *et al.*, Appl. Phys. A **70**, 33 (2000).
[28] G. Brauer *et al.*, Phys. Rev. B **54**, 2512 (1996).
[29] J. P. Perdew, K. Burke, and M. Ernzerhof, Phys. Rev. Lett. **77**, 3865 (1996).
[30] G. Kresse and J. Furthmüller, Phys. Rev. B **54**, 11 169 (1996).
[31] P. E. Blöchl, Phys. Rev. B **50**, 17 953 (1994).
[32] N. T. Son *et al.*, Phys. Rev. Lett. **96**, 055501 (2006).
[33] J. A. Chan, S. Lany, and A. Zunger, Phys. Rev. Lett. **103**, 016404 (2009).